Available online at www.sciencedirect.com
ScienceDirect
Computational Materials Science 44 (2008) 46–52
COMPUTATIONAL MATERIALS SCIENCE
www.elsevier.com/locate/commatsci

Structural and electronic properties of cubic HfO_2 surfaces

G.H. Chen, Z.F. Hou, X.G. Gong *

Surface Physics Laboratory and Department of Physics, Fudan University, Shanghai 200433, China

Available online 6 March 2008

Abstract

Using the first-principles method within the generalized gradient approximation, we have performed a systematic study on the structural and electronic properties of cubic HfO_2 surfaces. We find that the most energetically favorable surfaces are (1 1 0) and (1 1 1) terminated with single oxygen layer, both of which are stoichiometric. The atomic relaxation in top layers of surface (1 1 1)-O and (1 1 0) exhibits very similar behavior, i.e. cations relax inward while anions outward. This could be well understood by the ionic feature of the Hf–O bond. Both of the two surfaces studied are insulating without any surface state in the energy gap.

PACS: 68.35.Md; 68.47.Gh; 73.20.At; 81.10.Aj

Keywords: High κ; HfO_2; Surfaces; First-principles

1. Introduction

Hafnium dioxide (HfO_2) recently attracts much attention in the gate stack of metal oxide semiconductor field-effect transistors (MOSFETs) due to its relatively high dielectric constant, wide bandgap and good stability upon Si, and so on [1]. In 2006 it was reported hafnium based oxides was successfully employed as gate dielectric in 45 nm transistor technology by Intel [2]. However the performance of HfO_2 dielectric integrated into silicon technology is essentially determined by the upper interface between gate electrode and HfO_2 as well as the bottom interface between HfO_2 and Si channel. The study on surface properties of HfO_2 is preliminary and necessary for understanding the behavior of these two interfaces. In previous theoretical studies on interfaces of metal gate/HfO_2 [3,4], HfO_2/Si [5–8], and HfO_2/SiO_2 [9], the orientation of HfO_2 layers is mostly chosen as (0 0 1) surfaces based on the consideration of lattice matching. Although these modeling studies have successfully predicted some physical properties of interfaces, first-principles calculations on surface energies of monoclinic HfO_2 have shown that [10] ($\bar{1}$ 1 1) and (1 1 1) surfaces are thermodynamically favored surfaces while the (0 0 1) face is kinetically favored, which are also supported by the X-ray diffraction (XRD) spectra of HfO_2 thin films grown or annealed at different temperatures [11–15]. For gate stack of MOSFETs, HfO_2 gate dielectric must be thermodynamically stable on Si substrate. Therefore, in order to build more realistic model for interfaces related to HfO_2, a complete understanding of surface properties of HfO_2 film is required. Research work on this topic is still limited, and only monoclinic HfO_2 surfaces have been reported [10]. Furthermore, the effect of termination layer of surfaces on electronic structure of HfO_2 films was neglected in the work of Mukhopadhyay et al. [10]. However, an effective metallization of HfO_2 surface by heating to $T > 600\,^{\circ}C$ was detected by low energy ion spectroscopy in recent experimental study [16], suggesting that the termination of outmost surface layer significantly affects the surface electronic structures of HfO_2 films. It has been shown that the crystal field effects in HfO_2 polymorphs mainly result in the different width of lower conduction bands [17], therefore, we alternatively choose cubic phase of HfO_2 to detailedly

* Corresponding author.
E-mail address: xggong@fudan.edu.cn (X.G. Gong).

0927-0256/$ - see front matter © 2008 Elsevier B.V. All rights reserved.
doi:10.1016/j.commatsci.2008.01.051

understand the surface properties of HfO_2. In this work, first-principles calculations are performed to systematically study the atomic structures, stabilities, and electronic structures of low Miller index surfaces (i.e. (1 0 0), (1 1 0) and (1 1 1)) with various termination layers of cubic HfO_2.

This paper is organized as follows. The next section describes the computational details of this study. In the third section we discuss the bulk properties, surface energies, atomic relaxations of surfaces, and surface electronic structures of cubic HfO_2 as well. In the last section we draw some general conclusions.

2. Computational details

All simulations here are carried out using plane wave pseudopotential method as implemented in the Vienna *ab initio* simulation package (VASP) [18,19]. The exchange-correlation functional is treated within the generalized gradient approximation and parameterized by Perdew–Wang formula [20]. The interaction between ions and electrons is described by ultra-soft Vanderbilt pseudopotentials [21,22]. The wave functions are expanded in plane wave up to a cutoff energy of 495 eV. Brillouin-zone integrations are approximated by using the special k-point sampling of Monhkorst–Pack scheme [23]. Atomic relaxations are performed within the conjugated gradient scheme and the force on each atom is converged to be less than 0.01 eV/Å. For the electronic minimization the special Davison block iteration algorithm [24] is adopted and a tolerance of 0.02 meV for absolute difference of total energy is used during the electronic self-consistent loop. In the calculations of cubic HfO_2 bulk, a mesh size of $5 \times 5 \times 5$ is used for k-point sampling.

To model the surfaces of cubic HfO_2, we used the well-known "slab" approach, in which periodic boundary conditions are applied to the surface supercell including a slab of atomic layers and a vacuum region as shown in Fig. 1. In present work, we focus on the surface energies and corresponding local relaxations rather than the complex reconstructions, therefore, 1×1 unit cells are used for the low Miller index (i.e. (1 0 0), (1 1 0), and (1 1 1)) surfaces of cubic HfO_2 in our calculations. To guarantee surfaces on both sides of the slab being equivalent and eliminate the net dipole moment, we employ a slab with a mirror symmetry. For cubic HfO_2, its (1 0 0) surface may be terminated either by one atomic Hf or O layer (labeled as –Hf and –O, respectively), and its (1 1 1) surface could be terminated by one atomic Hf layer, one atomic O layer, or two atomic O layers (labeled as –Hf, –O, and –OO, respectively). The vacuum layer of 10 Å is enough to avoid the interactions between periodic slabs of atomic layers. 11 or 12 atomic layers are used in the slab for each case. The structures of supercells for the surfaces of cubic HfO_2 studied here are shown in Fig. 1. The k-meshes $11 \times 11 \times 1$, $8 \times 12 \times 1$, and $12 \times 12 \times 1$ are used in the calculations of (1 0 0), (1 1 0) and (1 1 1) surfaces of cubic HfO_2, respectively.

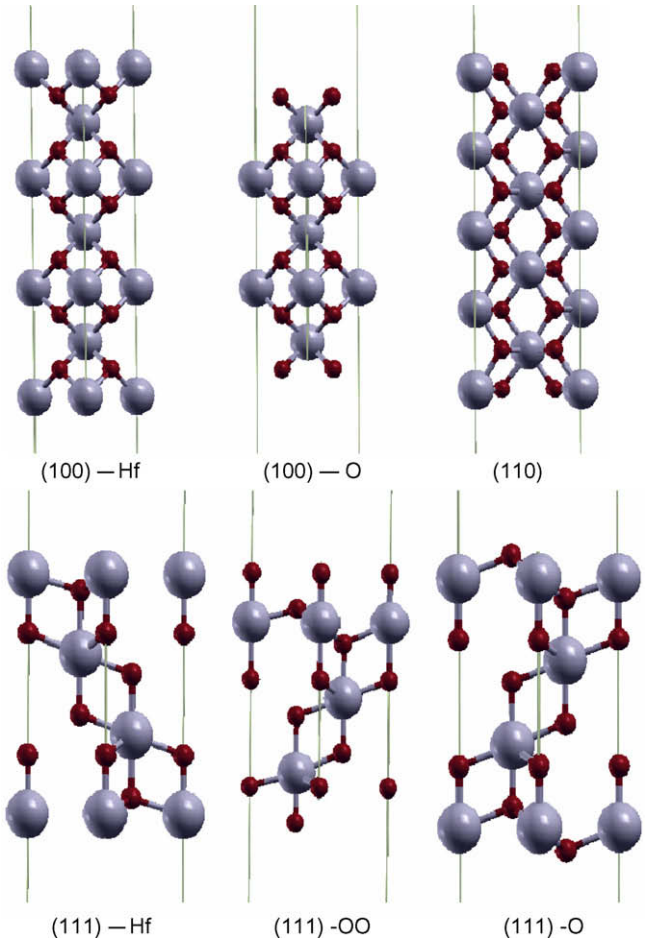

Fig. 1. The ball and stick model for the surface structures of cubic HfO_2. '–Hf', '–O', and '–OO' mean the surfaces are terminated by one Hf atom layer, one O atom layer, and two O atom layers, respectively. Big balls represent Hf atoms, and small ones for O atoms.

3. Results and discussions

3.1. Bulk properties

The lattice constant a of 5.06 Å and the bulk modulus B_0 of 261 GPa for cubic HfO_2 bulk are obtained in present work. Both of them are in good agreement with other calculation results [17,25] and available experimental value ($a_{expt} = 5.08$ Å) [26]. The density of states (DOS) of bulk cubic HfO_2 is shown in Fig. 2. The valence bands are split into two discontinuous groups. The lower part between −20 eV and −15 eV is mostly composed of O s states and the upper one mainly comes from O p states along with a fraction of Hf d states. While Hf d states mainly contribute to the conduction bands. It can also be seen that the valence band maximum (VBM) and the conduction band minimum (CBM) of bulk cubic HfO_2 mostly come from the O p states and Hf d states, respectively. Thus, our results indicate that Hf–O bonding in HfO_2 exhibits strong ionic characteristics with weak covalency. These are in good agreement with previously calculated results of cubic HfO_2 based on a variety of computational methods [27,28].

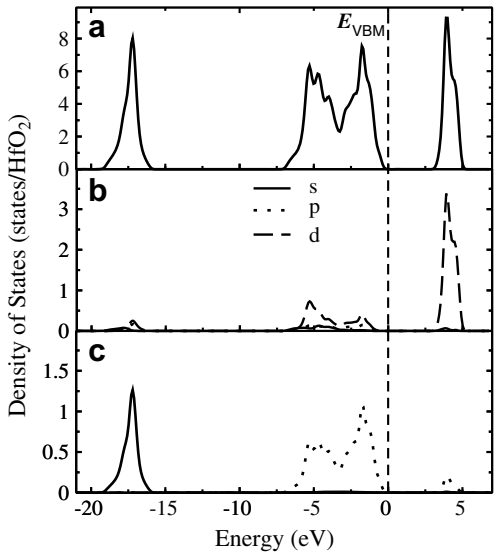

Fig. 2. (a) Total density of states (DOS) of cubic HfO_2, (b) partial DOS of Hf atom, and (c) partial DOS of O atom. E_{VBM} denotes the valence band maximum.

The bonding characteristics in cubic structure of HfO_2 is essentially similar to that in monoclinic HfO_2 [29], although the atomic coordinations are slightly different. In monoclinic structure, the oxygen atom is either threefold or fourfold coordinated, while all the Hf atoms are in a sevenfold-coordinated configuration [25,29]. In cubic phase, the coordination number of Hf is eight, while the O atom is fourfold coordinated [25]. Previous study on electronic structures of HfO_2 polymorphs suggests that the crystal field effects due to atomic coordinations mainly result in different width of lower conduction bands [17], thus we expect surface electronic structures of cubic HfO_2 discussed below could be extended to those of other phases.

3.2. Surface energies

To compare the stability of various surfaces, the surface energies (E^{surf}) should be taken into account. For HfO_2, E^{surf} is calculated as:

$$E^{surf} = \frac{1}{2A}\{E^{slab}_{tot} - N_{Hf}E^{HfO_2}_{tot} - (N_O - 2N_{Hf})\mu_O\}, \quad (1)$$

where E^{slab}_{tot} refers to the total energy of the slab supercell, $E^{HfO_2}_{tot}$ is the energy for bulk HfO_2 per formula unit (f.u.), and A is the surface area. N_{Hf} and N_O are numbers of Hf atoms and oxygen atoms in the slab, so the $(N_O - 2N_{Hf})$ equals to excessive oxygen beyond stoichiometric HfO_2 units in the slab. μ_O is the chemical potential of oxygen. In order to study the dependence of surface stability on the environment, μ_O is assumed to vary between thermodynamically allowed chemical potential μ^0_O and $\mu^{HfO_2}_O$, where μ^0_O is the chemical potential of oxygen and taken as half of total energy of one O_2 molecule, and $\mu^{HfO_2}_O$ is related with $\mu^{HfO_2}_{Hf}$ through

$$\mu^{HfO_2}_{Hf} + 2\mu^{HfO_2}_O = E^{HfO_2}_{tot}. \quad (2)$$

Because the formation energy ($\Delta E^{HfO_2}_f$) of bulk HfO_2 is defined as:

$$\Delta E^{HfO_2}_f = E^{HfO_2}_{tot} - \mu^0_{Hf} - 2\mu^0_O, \quad (3)$$

where μ^0_{Hf} is the chemical potential of Hf and taken as the total energy of bulk Hf per f.u., we can obtain the variation range of μ_O:

$$\mu^0_O + \frac{1}{2}\Delta E^{HfO_2}_f \leqslant \mu_O \leqslant \mu^0_O. \quad (4)$$

The calculated surface energies for low Miller index surfaces of cubic HfO_2 are listed in Table 1. Both the values of surface energies before and after structural relaxation are listed for comparison, and the change of surface energies due to relaxation is given by $\%\Delta E^{surf}$. $\%\Delta E^{surf}$ is defined as [30],

$$\%\Delta E^{surf} = [E^{surf}_{relaxed} - E^{surf}_{unrelaxed}]/E^{surf}_{unrelaxed}, \quad (5)$$

where $E^{surf}_{unrelaxed}$ and $E^{surf}_{relaxed}$ are the surface energies before and after structural relaxation, respectively. It can be seen that the surface energies of all low Miller index surfaces of cubic HfO_2 are decreased by structural relaxation. The variation order of the absolute value of surface energies of cubic HfO_2 due to structural relaxation is: (110) > (111)-OO > (100)-O > (100)-Hf > (111)-Hf > (111)-O. Obviously the surface energy of (110) surface changes most drastically. In order to compare the stability of surfaces of cubic HfO_2, the surface energies of relaxed (100)-Hf, (100)-O, (110), (111)-Hf, (111)-OO, and (111)-O surfaces versus the chemical potential of oxygen are plotted in Fig. 3. Under oxygen-rich conditions the stability of low Miller index surfaces of cubic HfO_2 follows in the sequence as: (111)-O > (110) > (100)-O > (111)-OO > (100)-Hf > (111)-Hf, while under oxygen-deficient conditions it changes to: (111)-O > (110) > (100)-Hf > (111)-Hf > (100)-O > (111)-OO. It indicates that (111)-O and (110) are the most stable surfaces. This is basically similar to surfaces of cubic ZrO_2 with same structure of HfO_2. The unrelaxed surface energies of (100), (110) and (111) surfaces of cubic ZrO_2 have been calculated by Christensen and Carter [31], they found that (111) surface

Table 1
Calculated surface energies E^{surf} (mJ/m^2) for low-index surfaces of cubic HfO_2

Face	$E^{surf}(\mu_O = \mu^0_O)$			$E^{surf}(\mu_O = \mu^0_O + \frac{1}{2}\Delta E^{HfO_2}_f)$		
	Relaxed	Unrelaxed	$\%\Delta E^{surf}$	Relaxed	Unrelaxed	$\%\Delta E^{surf}$
(100)-Hf	2650	2808	5.63	9353	9511	1.66
(100)-O	10175	10410	2.26	3472	3707	6.34
(110)	1526	2230	31.6	1526	2230	31.6
(111)-Hf	2673	2811	4.91	10416	10554	1.31
(111)-OO	12537	12916	2.93	4794	5172	7.31
(111)-O	934	996	6.22	934	996	6.22

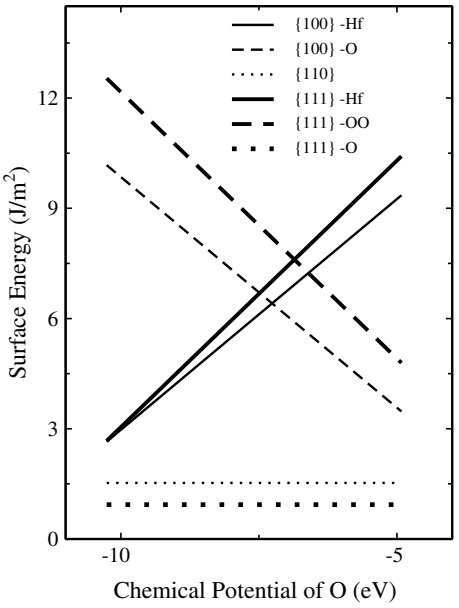

Fig. 3. Surface energies for various surfaces of cubic HfO_2 versus chemical potential of oxygen.

of cubic ZrO_2 is the most stable one. These could be understood by that (1 1 1) surfaces of cubic HfO_2 and ZrO_2 satisfy the compactness and electrostatic conditions [31]. In addition, because the (1 1 1)-O and (1 1 0) surfaces of cubic HfO_2 are stoichiometric, their surface energies are independent of the variation of chemical potential of oxygen.

3.3. Surface relaxation

In present work, we focus on the atomic relaxation along the surface normal and neglect the reconstruction. Since the (1 1 1)-O and (1 1 0) surfaces of cubic HfO_2 are energetically the most stable ones as discussed in above section, here we particularly present and discuss the atomic relaxations in these two surfaces.

To obtain the detailed information of atomic relaxation in each atomic layer, we calculate the absolute displacement Δz of each atomic layer and the change of layer distance Δd. During our calculations, the surface normal was chosen as the z-axis. Here, the Δz is given by $\Delta z = z^{\text{relaxed}} - z^{\text{unrelaxed}}$, where $z^{\text{unrelaxed}}$ and z^{relaxed} are z coordinates of atom before and after relaxation, respectively. If

Table 2
Atomic relaxation in (1 1 0) surface of cubic HfO_2

n	Δz_n		$\Delta d_{n,n+1}$		$z_n^{\text{O}} - z_n^{\text{Hf}}$
	Hf	O	Hf	O	
1	−0.225	0.049	−0.408	0.053	0.274
2	0.183	−0.004	0.243	−0.012	−0.187
3	−0.06	0.008	–	–	0.068

n is layer number, Δz_n (Å) is the absolute displacement of atom along z-direction and $\Delta d_{n,n+1}$ (Å) denotes change of distance between layer n and $n+1$ due to relaxation. $z_n^{\text{O}} - z_n^{\text{Hf}}$ (Å) denotes the rumpling of Hf and O atoms layers.

Table 3
Atomic relaxations in (1 1 1)-O surface of cubic HfO_2

n	Atom	Δz_n	$\Delta d_{n,n+1}$
1	O	0.032	0.068
2	Hf	−0.035	−0.005
3	O	−0.03	−0.048
4	O	0.018	0.007
5	Hf	0.011	–

n is layer number, Δz_n (Å) is the displacement of atom along z-direction (the positive indicates atoms move outward and the negative means inward) and $\Delta d_{n,n+1}$ (Å) denotes change of distance between layer n and $n+1$ due to relaxation.

Δz is negative, it indicates that atom moves toward the inner layer by relaxation, otherwise, atom moves toward outer layer. We should point out that two or three atomic layers in center part of the slab are fixed during the structural relaxations in our calculations. Δd is defined as the difference between d^{relaxed} and $d^{\text{unrelaxed}}$ (i.e. $\Delta d = d^{\text{relaxed}} -$

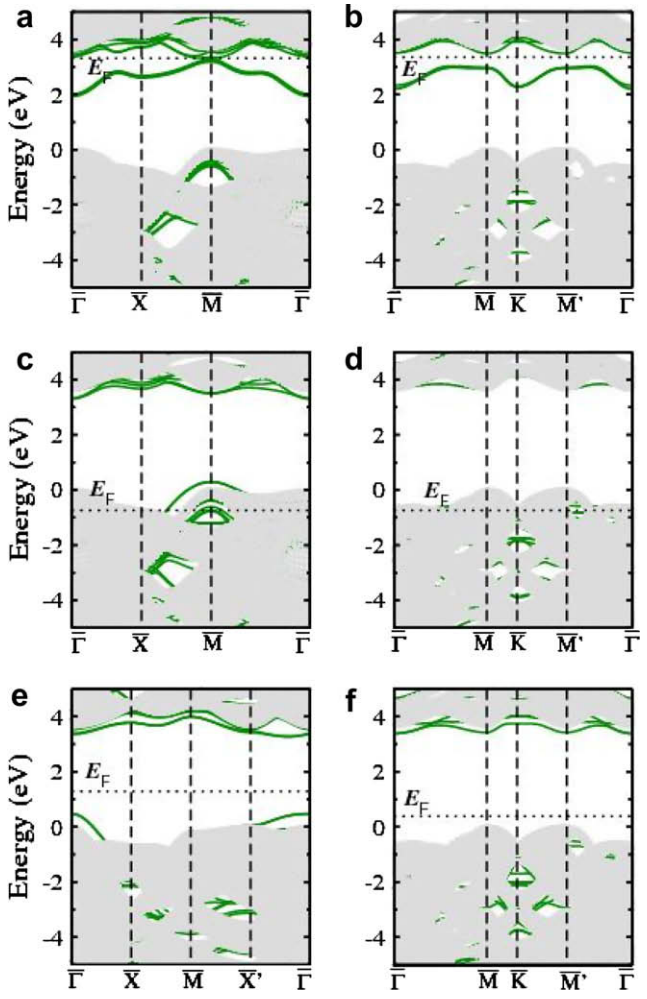

Fig. 4. Projected bulk band structures of various surfaces: (a) Hf-terminated (1 0 0), (b) Hf-terminated (1 1 1), (c) O-terminated (1 0 0), (d) double O atom layer terminated (1 1 1) surface, (e) (1 1 0) and (f) one O atom layer terminated (1 1 1). The position of the Fermi level E_F of surface is marked by the dotted line.

$d^{\text{unrelaxed}}$), where d^{relaxed} and $d^{\text{unrelaxed}}$ are the distances between two neighboring layers in relaxed and unrelaxed surfaces, respectively. If Δd is positive, it indicates that atomic layer distance in surfaces is increased by relaxation. The absolute displacement of each atomic layer and the change of layer distance in (1 1 0) and (1 1 1)-O surfaces of cubic HfO_2 are listed in Tables 2 and 3, respectively. For (1 1 0) surface of cubic HfO_2, each atomic layer is stoichiometric and nonpolar because the ratio of Hf:O in each lay is 1:2. As listed in Table 2, Hf atoms in the first top layer move inward and those in the second top layer outward due to the relaxation. Consequently the relaxation results in the atomic layer distance between the first and second top Hf atom layers ($\Delta d^{\text{Hf}}_{1,2}$) decreased (see Table 2). The O atoms in the first and second top layers move outward and inward by relaxation, respectively, which are different from that of Hf atoms. This means that the atomic layer distance between the first and second top O atom layers is increased ($\Delta d^{\text{O}}_{1,2}$) (see Table 2) by relaxation. While the atomic layer distance between the second and third Hf atom layers ($\Delta d^{\text{Hf}}_{2,3}$) is increased, $\Delta d^{\text{O}}_{2,3}$ decreased. All of above results clearly demonstrate a trend of rumpling, which is common in some ionic crystals, appears in (1 1 0) surface of cubic HfO_2. In order to make this clear, we also list the rumpling between Hf atom layer and O atom layer (defined as $z^{\text{O}}_n - z^{\text{Hf}}_n$) due to relaxation in Table 2. The first top layer exhibits the strongest rumpling.

For the (1 1 1)-O surface, the first top layer only contains O atoms and which move outward by relaxation. The second top layer only contains Hf atoms which move inward. Consequently the layer distance between the first and second top layers (Δd_{12}) is increased by relaxation (see Table 3). There are only O atoms in the third top layer, in which the O atoms move inward and the layer distance between the second and third layers (Δd_{23}) is slightly decreased by relaxation. In addition, our results indicate both of the O atoms in the fourth top layer and the Hf atoms in the fifth top layer move outward. But the absolute value of displacement of the former is slightly larger, corresponding to a layer distance increase by relaxation.

Actually, no matter atoms move inward or outward due to relaxation, atomic relaxation in these surfaces of cubic HfO_2 could be well understood by the ionic characteristics of Hf–O bonding. When the surface is formed by cleaving a crystal, the balance of forces exerting on anions or cations in outmost layers of HfO_2 surface is broken, resulting in the redistribution of the electrons. In this way the ions are polarized. As the anions have larger polarizability and volumes than the cations, they undergo larger forces from the dipole induced by the electrons and relax outward. In contrast, the top layer cations is apt to move inward. As a result, rumpling occurs, i.e. the electrical double layer can be formed to make the surface energy lower.

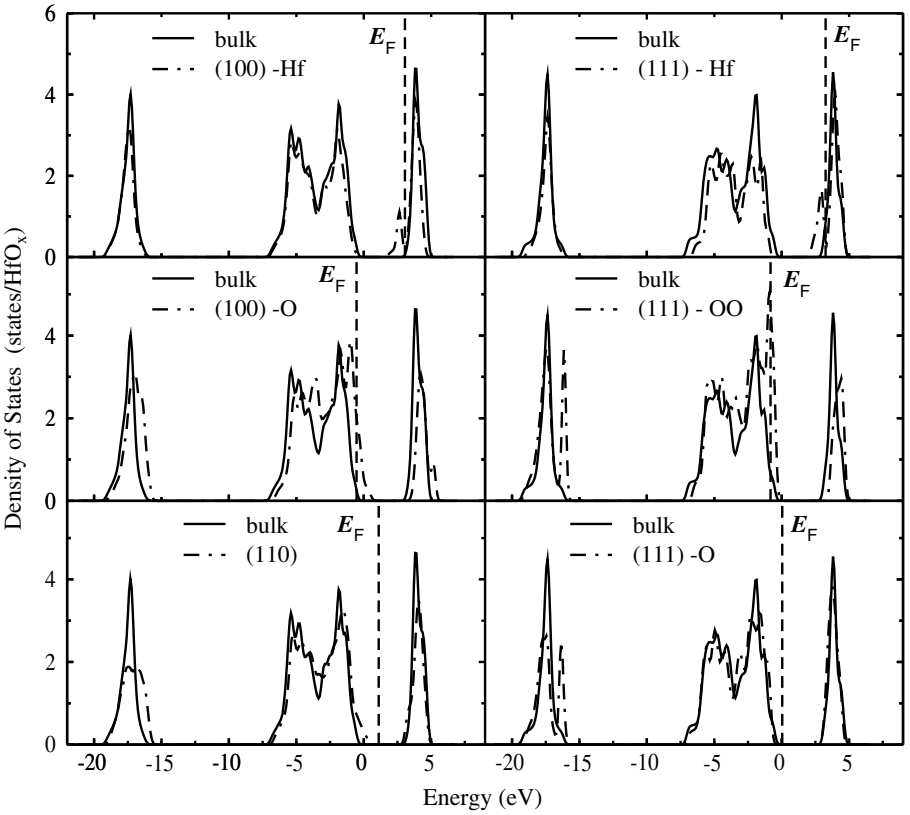

Fig. 5. Density of states of surfaces. For comparison, valence band maximum (VBM) of cubic HfO_2 bulk has been aligned at zero. The Fermi level of each surface is marked by the dashed line.

3.4. Electronic properties

In this section, we turn to discuss the electronic structures of cubic HfO_2 surfaces. The projected band structures of (100)-Hf, (111)-Hf, (100)-O, (111)-OO, (110) and (111)-O surfaces are shown in Fig. 4. For Hf-terminated surfaces, i.e. (100)-Hf and (111)-Hf, there are occupied surface states within the band gap of bulk cubic HfO_2. The (100)-Hf and (111)-Hf surfaces can hence exhibit metallic properties. For (100)-O and (111)-OO surfaces, empty surface states occur in the vicinity of valence band maximum (VBM) of bulk cubic HfO_2 and the Fermi level is located in the valence bands of cubic HfO_2. It indicates that (100)-O and (111)-OO surfaces also exhibit metallic properties. The (110) surface and (111) surface terminated by one atomic O layer still exhibit insulating properties without surface states in the energy gap of bulk cubic HfO_2. This suggests that the growth of (110) surface and (111) surface terminated with one atomic O layer of cubic HfO_2 on Si substrate could achieve good electric performance.

In order to explore the characteristics of surface states, we calculate the density of states (DOS) for each surface. The total DOS of each surface are shown in Fig. 5, in which the VBM of the cubic HfO_2 is set as the energy zero and the partial DOS of atom in the center of slab of each surface is aligned with that of the corresponding atom in bulk cubic HfO_2. For Hf-terminated (100) and (111)surfaces, the surface states appear between the CBM of cubic HfO_2 and the Fermi level, in consistent with above projected band structures. Both the (100) and (111) surfaces terminated with Hf are non-stoichiometric and Hf is excessive. These surface states are contributed by d states of surface Hf cations and hence come from conduction bands. For O terminated non-stoichiometric surfaces (100) and (111)-OO, surface states appear near the VBM of bulk cubic HfO_2 and are mainly contributed by p states of surface oxygen anions. (110) and (111)-O surfaces are stoichiometric and there are no surface states within the energy gap. In recent experiment [16], the surface electronic structures of HfO_2 films were detected by low energy ion spectroscopy and the effective metallization of HfO_2 surface under heating to $T > 600\,^{\circ}C$ was observed. The authors [16] ascribed the formation of a metal-like band on the surface of HfO_2 to the generation of a large number of defects with their electronic states in the band gap which was believed to result from the oxygen desorption and oxide reduction in the outmost surface layer. Our calculated surface electronic structures of cubic HfO_2 suggest that the experimentally probed HfO_2 surfaces could be the ones terminated by Hf atom layers.

4. Conclusions

The structural and electronic properties of cubic HfO_2 surfaces have been investigated by the first-principles calculations at atomic scale. We find that both surface energies and electronic structures of surfaces of cubic HfO_2 significantly depend on the ratio of Hf:O. It indicates the thermal treatment of HfO_2 films can greatly affect the surfaces electronic structures of cubic HfO_2. Hf-terminated surfaces of cubic HfO_2 exhibit metallic properties, which is in consistent with the observation in recent experiment [16]. Stoichiometric surfaces tend to be energetically stable and show good insulating properties, such as (110) and (111)-O surfaces. Due to the ionic feature of Hf–O bond, the rumpling occurs in (110) surface of cubic HfO_2.

Acknowledgements

This work is partially supported by the NSF of China (Grant no. 10674028), the national program for the basic research and research project of Shanghai. The computation was performed at Shanghai Supercomputer Center and Supercomputer Center of Fudan.

References

[1] G.D. Wilk, R.M. Wallace, J.M. Anthony, J. Appl. Phys. 89 (2001) 5243.
[2] Intel, Meet the world's first 45 nm processor, see for example, <http://www.intel.com/technology/silicon/45nm_technology.htm> (January 2006).
[3] A.A. Knizhnik, A.A. Safonov, I.M. Iskandarova, A.A. Bagatur'yants, B.V. Potapkin, L.R.C. Fonseca, M.W. Stoker, J. Appl. Phys. 99 (2006) 084104.
[4] A.V. Gavrikov, A.A. Knizhnik, A.A. Bagatur'yants, B.V. Potapkin, L.R.C. Fonseca, M.W. Stoker, J. Schaeffer, J. Appl. Phys. 101 (2007) 014310.
[5] V. Fiorentini, G. Gulleri, Phys. Rev. Lett. 89 (2002) 266101.
[6] R. Puthenkovilakam, J.P. Chang, J. Appl. Phys. 96 (2004) 2701.
[7] P.W. Peacock, J. Robertson, Phys. Rev. Lett. 92 (2004) 057601.
[8] P.W. Peacock, K. Xiong, K. Tse, J. Robertson, Phys. Rev. B 73 (2006) 075328.
[9] O. Sharia, A.A. Demkov, G. Bersuker, B.H. Lee, Phys. Rev. B 75 (2007) 035306.
[10] A.B. Mukhopadhyay, J.F. Sanz, C.B. Musgrave, Phys. Rev. B 73 (2006) 115330.
[11] M.Y. Ho, H. Gong, G.D. Wilk, B.W. Busch, M.L. Green, P.M. Voyles, D.A. Muller, M. Bude, W.H. Lin, A. See, M.E. Loomans, S.K. Lahiri, P.I. Räisänen, J. Appl. Phys. 93 (2003) 1477.
[12] D. Triyoso, R. Liu, D. Roan, M. Ramon, N.V. Edwards, R. Gregory, D. Werho, J. Kulik, G. Tam, E. Irwin, X.D. Wang, L.B. La, C. Hobbs, R. Garcia, J. Baker, B.E. White, P. Tobin, J. Electrochem. Soc. 151 (2004) 220.
[13] J. Aarik, A. Aidla, H. Mändar, V. Sammelselg, T. Uustare, J. Cryst. Growth 220 (2000) 105.
[14] J. Aarik, H. Mändar, M. Kirm, L. Pung, Thin Solid Films 466 (2004) 41.
[15] K. Kukli, J. Aarik, M. Ritala, T. Uustare, T. Sajavaara, J. Lu, J. Sundqvist, A. Aidla, L. Pung, A. Hårsta, M. Leselä, J. Appl. Phys. 96 (2004) 5298.
[16] A. Zenkevich, Y. Lebedinskii, M. Pushkin, V. Nevolin, Appl. Phys. Lett. 89 (2006) 172903.
[17] J.E. Jaffe, R.A. Bachorz, M. Gutowski, Phys. Rev. B 72 (2005) 144107.
[18] G. Kresse, J. Furthmüller, Comput. Mater. Sci. 6 (1996) 15.
[19] G. Kresse, J. Furthmüller, Phys. Rev. B 54 (1996) 11169.
[20] J.P. Perdew, J.A. Chevary, S.H. Vosko, K.A. Jackson, M.R. Pederson, D.J. Singh, C. Fiolhais, Phys. Rev. B 46 (1992) 6671.
[21] D. Vanderbilt, Phys. Rev. B 41 (1990) 7892.
[22] G. Kresse, J. Hafner, J. Phys.: Condens. Mat. 6 (1994) 8245.

[23] H.J. Monkhorst, J.D. Pack, Phys. Rev. B 13 (1976) 5188.
[24] E.R. Davison, in: G.H.F. Diercksen, S. Wilson (Eds.), Methods in Computational Molecular Physics, NATO Advanced Study Institute, Series C, vol. 113, Plenum, New York, 1983.
[25] J. Kang, E.C. Lee, K.J. Chang, Phys. Rev. B 68 (2003) 054106.
[26] J. Wang, H.P. Li, R. Stevens, J. Mater. Sci. 27 (1992) 5397.
[27] M.A. Caravaca, R.A. Casali, J. Phys.: Condens. Mat. 17 (2005) 5795.
[28] R. Terki, H. Feraoun, G. Bertrand, H. Aourag, Comput. Mater. Sci. 33 (2005) 44.
[29] A.S. Foster, F.L. Gejo, A.L. Shluger, R.M. Nieminen, Phys. Rev. B 65 (2002) 174117.
[30] A.L. Rosa, J. Neugebauer, Phys. Rev. B 73 (2006) 205346.
[31] A. Christensen, E.A. Carter, Phys. Rev. B 58 (1998) 8050.